Korean J. Chem. Eng., 33(12), 3493-3503 (2016)
DOI: 10.1007/s11814-016-0211-6

pISSN: 0256-1115
eISSN: 1975-7220

Experimental solubility and absorption mechanism of dilute SO_2 in aqueous diethylene glycol dimethyl ether solution

Qiuxia Xu*, Jianbai Xiao, Jianbin Zhang*,†, and Xionghui Wei**,†**

*College of Chemical Engineering, Inner Mongolia University of Technology, Huhhot 010051, China
**Department of Applied Chemistry, College of Chemistry & Molecular Engineering, Peking University, Beijing 100871, China
(*Received 2 April 2016 • accepted 18 July 2016*)

Abstract−SO_2 absorption capabilities of DEGDME+H_2O system with different compositions were systemically investigated. The DEGDME+H_2O system exhibited superior SO_2 absorption capability and optimal desorption property with a desorption rate of higher than 94% under the desorption conditions. In addition, it has been demonstrated that the DEGDME+H_2O system possessed remarkable SO_2 absorbing and releasing capability after multiple recycles. Moreover, GLE data were measured for dilute SO_2 in the system of DEGDME+H_2O, in which SO_2 partial pressures were determined in the range of 0 to 140 Pa. By fitting of GLE data, HLC, ΔH, ΔS and ΔG of SO_2 absorption process were obtained. UV, FTIR, ^{1}H-NMR, and ^{13}C-NMR spectra of absorbing systems in the SO_2 absorption processes were studied to elucidate the absorption mechanism. On the basis of the spectral results, the intermolecular hydrogen bonding and S…O interaction between SO_2 with the absorption system were discussed.

Keywords: Gas-liquid Equilibrium, Diethylene Glycol Dimethyl Ether, SO_2, Thermodynamic Parameter, Absorption Mechanism

INTRODUCTION

SO_2 is a major atmospheric pollutant since its emission is directly related to the consumption of fossil fuels and burning of biomass. The emissions of SO_2 cause a variety of significant adverse impacts on human health and the global environment. Therefore, the efficient removal of SO_2 from flue gases has become an increasingly important environmental challenge and demand. Flue gas desulfurization (FGD) techniques [1-3], including wet FGD, dry FGD, and semi-dry FGD processes, have been widely applied to reduce the emission of SO_2. However, the most widespread lime or limestone scrubbing procedure produces large volumes of solid waste, such as calcium sulfate, which needs to be treated further. Alternatively, one of the most attractive approaches for separating SO_2 from flue gasses is absorption by organic solvent [4-11], which has demonstrated favorable properties for absorption and desorption of acid gasses [12-14].

Organic solvents have been identified as optimal absorbents for their low vapor pressure, low toxicity, high chemical stability, and low melting point. Among the numerous organic solvents, ether solvents exhibit favorable absorption and desorption capabilities for the removal of acid gases [15-18]. A survey of the literature revealed that the GLE data for SO_2 in diethylene glycol dimethyl ether (DEGDME)+water (H_2O) [19-25] system have not been studied up to the present, although they are critical for the design and operation of the absorption and desorption processes using such liquid systems.

Herein, we mainly focused on providing gas-liquid equilibrium (GLE) data for dilute SO_2 in the binary system DEGDME (1)+H_2O (2) at T=(298.15, 303.15, 308.15, 313.15, and 318.15) K and p=122.7 kPa. We calculated the HLC, ΔG, ΔH, and ΔS of SO_2 absorption in diethylene glycol dimethyl ether (DEGDME)+water (H_2O) system on the basis of the measured GLE data. In addition, intermolecular hydrogen bonding and S…O interaction of the system DEGDME and H_2O with SO_2 were analyzed and discussed using UV, FTIR, ^{1}H-NMR, and ^{13}C NMR spectral techniques. The results of this work provide important basic data for the design and operation of the absorption and desorption processes in industrial scale FGD processes.

EXPERIMENTAL

1. Materials

The analytical grade DEGDME was purchased from Sinopharm Chemical Reagent Co., Ltd. It was dried using molecular sieves (type 4A) and degassed ultrasonically before using. The purity of the sample was checked by density determination at T=298.15 K [26]. The density of DEGDME at 298.15 K was found to be 0.9398 g·cm^{-3}, which is in good agreement with the literature values of 0.9392 g·cm^{-3} [9] and 0.9399 g·cm^{-3} [27]. The certified standard mixture (SO_2+N_2, y_{SO_2}=0.01) was used to determine the GLE data for DEGDME (1)+H_2O (2) system with dilute SO_2, which was purchased from the Beijing Oxygen Plant Specialty Gases Institute Company (China). Solutions of I_2 and $Na_2S_2O_3$ were used as standard solutions and distilled water was used to make the mixture solutions. Specification of chemical samples is listed in Table 1.

2. Apparatus and Experimental Procedure

GLE data for the system DEGDME (1)+H_2O (2) with SO_2 were

†To whom correspondence should be addressed.
E-mail: xhwei@pku.edu.cn, tadzhang@pku.edu.cn

Table 1. Specification of chemical samples

Chemical name	Soure	Initial mass fraction/purity[a]	Purification method
Diethyl glycol dimethyl ether (DEGDME)	Sinopharm Chemical Reagent Co., Ltd.	≥0.995	Desiccation[b] and degasification[c]
Iodine (I_2)	Tianjin Yongsheng Fine Chemical Reagent Co., Ltd.	≥0.985	None
Sodium thiosulfate ($Na_2S_2O_3$)	Tianjin Yongsheng Fine Chemical Reagent Co., Ltd.	≥0.990	None
Potassium dichromate ($K_2Cr_2O_7$)	Shanghai Reagent Factory the second branch	≥0.998	393 K to dry 10 h
Double distilled water (H_2O)	Secondary distillation by College of Chemistry and Molecular Engineering, Peking university	0.990	Oscillation degassing

[a]Declared by the supplier
[b]Molecular sieve type 4A
[c]Ultrasound

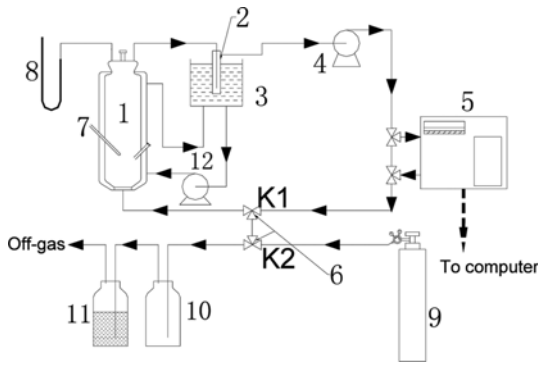

Fig. 1. Experimental setup of GLE measurement.

1. Jacketed vessel
2. Cold trap
3. Thermostatic bath
4. Gas circulatory pump
5. GC
6. Regulating valve
7. Thermometer
8. Pressure meter
9. SO_2+N_2 gas cylinder
10. Buffer
11. Waster gas treating bottle
12. Temperature-stabilizing water circulatory pump

obtained using a dynamic analytic method, and the apparatus is given in Fig. 1, which was based on the previous work [10].

In this work, only the gas mixture (SO_2/N_2) was recycled by a gas circulatory pump (4) (type: PCF 5015 N-24 V; flow rate: 15 L·min^{-1}; vacuum degree: 50 kPa. KV: 24 V, DC. Manufacturer: Chengdu Weichengkeji Co., Ltd., Chengdu, China). The concentrations of SO_2 in the gas phase were determined using a gas chromatograph (Agilent 6890N) equipped with a 2 m×3.2 mm Porapak Q packed column, an FPD detector, and an HP6890 workstation. To determine the relationship between concentrations of SO_2 and the response values of gas chromatograph, a calibration curve was constructed using an external standard method. Before experiment, the liquid used as absorbent was first put into the absorption bottle (1). Second, the mixture gas (SO_2/N_2) from gas cylinder (9), through switching the regulating valves K1 and K2 (6), was poured into the bottom of absorption bottle and contact fully with the liquid. The residual gases out of absorption bottle were recycled by a gas circulatory pump to be absorbed more adequately and quickly by the solution, and only a small fraction was used for the online quantitative test of SO_2 content at the same time. When the peak area responding to the concentration of SO_2 changed no longer with time, we considered equilibrium to be obtained. Meanwhile, the peak areas were recorded, and the just enough liquid samples were taken from absorption bottle to measure the concentration of SO_2 dissolved in the liquid phase. After one GLE experiment was performed, the mixture gas was discharged out by switching the regulating valve (6) and passing buffer (10) and waster gas treating bottle containing alkaline solution (11). A series of GLE data were gained by repeating operation above. During the experimental process, liquid temperatures were controlled using the thermostatic bath (3) and inspected by a standard thermometer (7) with the standard uncertainty u(T)=0.01 K. System pressures were inspected with a pressure meter (8) which had the standard uncertainty u(p)=0.10 kPa.

After the GLE experiments, the solutions which contained SO_2 were removed to the absorption bottle. Under atmospheric pressure, the mixture dissolving SO_2 was treated with gas stripping at T=308.15 K and T=393.15 K (In industry, desorption processes are performed using the stream extraction method at T=393.15 K), respectively. And N_2 was used as the carrier gas with 1 L·min^{-1}. After desorption, the GLE data of SO_2 in the regenerated solution were measured to determine the property of dissolving SO_2 based on the previous work [10]. The measurements of desorption and absorption of SO_2 were repeated at least three times.

UV-vis spectra were recorded on a Shimadzu UV-3150 spectrophotometer. Fourier transform infrared (FTIR) spectra were recorded on a Bruker Vector 22 spectrometer with 1 cm^{-1} resolution in the range from (4,000 to 400) cm^{-1}. The spectrometer possesses auto-align energy optimization and a dynamically aligned interferometer, and fitted with two constringent ZnS pellets for the measurement of aqueous solution, an OPUS/IR operator, and IR source. A baseline correction was made for the spectra, which were recorded in air, and then, 15 μL of solution was used on the FTIR spectrometer for every measurement, and the thin layer of samples was less than 2 μm (typical thicknesses). ^{1}H-NMR and ^{13}C-NMR spectra were acquired using an AVANCE III Bruker-500 MHz nuclear magnetic resonance spectrometer, and $CDCl_3$-d_1 was used as an NMR solvent. All experiments of DEGDME+SO_2 were performed at room temperature and atmospheric pressure.

3. Data Treatment

Sulfur (IV) concentration in the liquid phase (C_{SO_2}, mol·kg^{-1}) was determined by adding a known volume of liquid sample to another known volume of standard iodine solution. The excess iodine solution was back-titrated with the standard sodium thiosulfate solution [28]. At the same time, a blank experiment was also done, which was an improvement in comparison with the reported method [29]. Each experimental value was an average of at least three measurements.

C_{SO_2} was calculated from the following formula,

$$C_{SO_2}=1000C_{Na_2S_2O_3}(V_1-V_2)/(2V_3) \quad (1)$$

where $C_{Na_2S_2O_3}$ is the concentration of standard sodium thiosulfate solution ($Na_2S_2O_3$, mol·L^{-3}), V_1 is the volume of $Na_2S_2O_3$ solution consumed in blank experiment, V_2 is the volume of $Na_2S_2O_3$ solution consumed in real sample, V_3 is the volume of the determined liquid sample, and all units of volume are represented with milliliter. The GLE data were obtained with the relative expanded uncertainties (level of confidence=0.95, k=2) of $U_r(C_{SO_2})=\pm0.60\%$ for SO_2 concentration in the liquid phase and $U_r(y_{SO_2})=\pm2.50\%$ for SO_2 concentration in the gas phase.

In the experimental processes, the partial pressure of SO_2 (p_{SO_2}) in the gas phase was given by

$$p_{SO_2}=p\times y_{SO_2} \quad (2)$$

where p denotes the total pressure and p_{SO_2} denotes the volume fraction of SO_2 in the gas phase. y_{SO_2} was the volume fraction of SO_2.

For a gas substance, its solubility in a liquid could be generally described in terms of Henry's law, which was defined as [30-32],

$$H'=C_l/C_g \quad (3)$$

For a gas substance, its solubility in a liquid could be generally described in terms of Henry's law, which was defined as [30-32],

$$HLC=C_l/C_g \quad (4)$$

where C_l is the molality concentration of gas dissolved in the liquid phase with the units of Pa·kg·mol^{-1}, C_g is the molality concentration of SO_2 in the gas phase with the units of kg·mol^{-1}, HLC is the Henry's law constant with the units of Pa. HLC could be calculated by the linear slope of the GLE curves. Yet, HLC was equal to the limiting slope as the pressure (or solubility) approaches zero for SO_2 in other mixtures.

For these systems with the GLE curves being linear, the phase equilibrium equation of SO_2 was described as follows:

$$SO_2(g) \overset{K}{\rightleftharpoons} SO_2(L) \quad (5)$$

The equilibrium constant (K) was expressed as follows:

$$K=C_{SO_2}/p_{SO_2} \quad (6)$$

where C_{SO_2} is the SO_2 concentration dissolved in the liquid phase. So the HLC value was the reciprocal of dimensionless equilibrium constant. The standard Gibbs free energy change (ΔG) when SO_2 reached phase equilibrium could be expressed as follow,

$$\Delta G=-RT\ln(1/HLC) \quad (7)$$

Based on Van't Hoff equation:

$$\Delta G=\Delta H-T\Delta S \quad (8)$$

From Eqs. (6) and (7), it can be obtained from the following expression,

$$\ln HLC=\Delta H/RT-\Delta S/R \quad (9)$$

where ΔG denotes the standard Gibbs free energy of phase transition when phase equilibrium is reached, and ΔH (kJ·mol^{-1}) and ΔS (J·mol^{-1}·K^{-1}) are the enthalpy and entropy of the phase change from the dissolved phase to the gas phase, respectively. ln H′ vs. 1/T could be plotted, and ΔH and ΔS were obtained from the slope and the intercept after H′ was calculated at different temperatures.

RESULTS AND DISCUSSION

1. GLE Data for DEGDME+H_2O with Dilute SO_2

At T=308.15 K and p=122.7 kPa, a series of GLE data for the

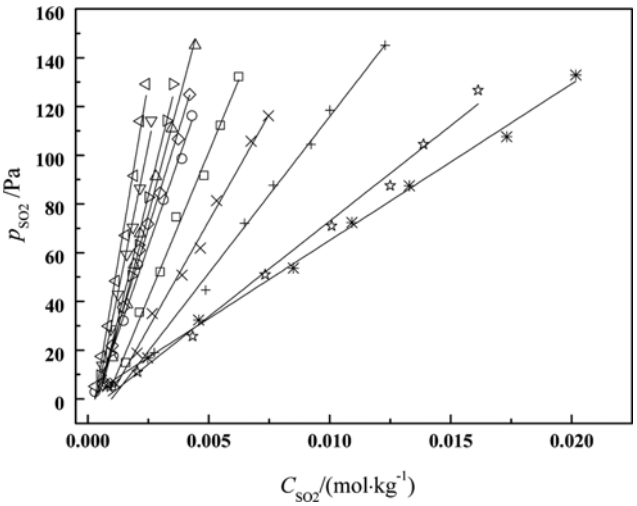

Fig. 2. GLE Curves for DEGDME+H_2O+SO_2+N_2 at T=308.15 K under p=122.7 kPa: □, w_1=0.00; ○, w_1= 0.10; △, w_1=0.20; ▽, w_1=0.30; ◁, w_1=0.40; ▷, w_1=0.50; ◇, w_1=0.60; ×, w_1= 0.70; +, w_1=0.80; ☆, w_1=0.90; and ✳, w_1=1.00.

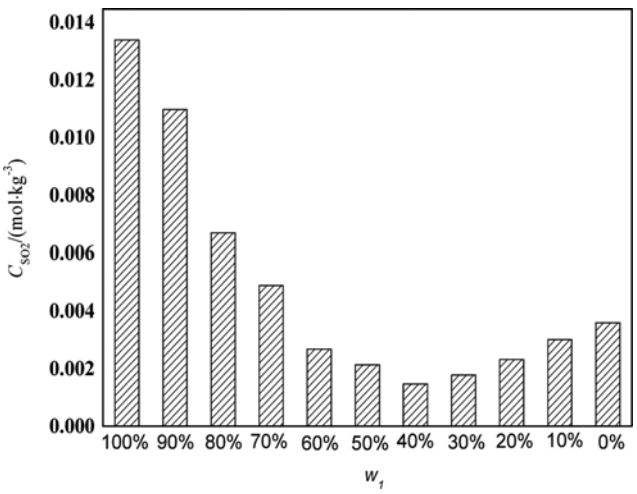

Fig. 3. Solubility of SO_2 in DEGDME+H_2O when SO_2 concentration in the gas phase was designed at. w_1 refers to the mass fraction of DEGDME in mixed solution (DEGDME+H_2O).

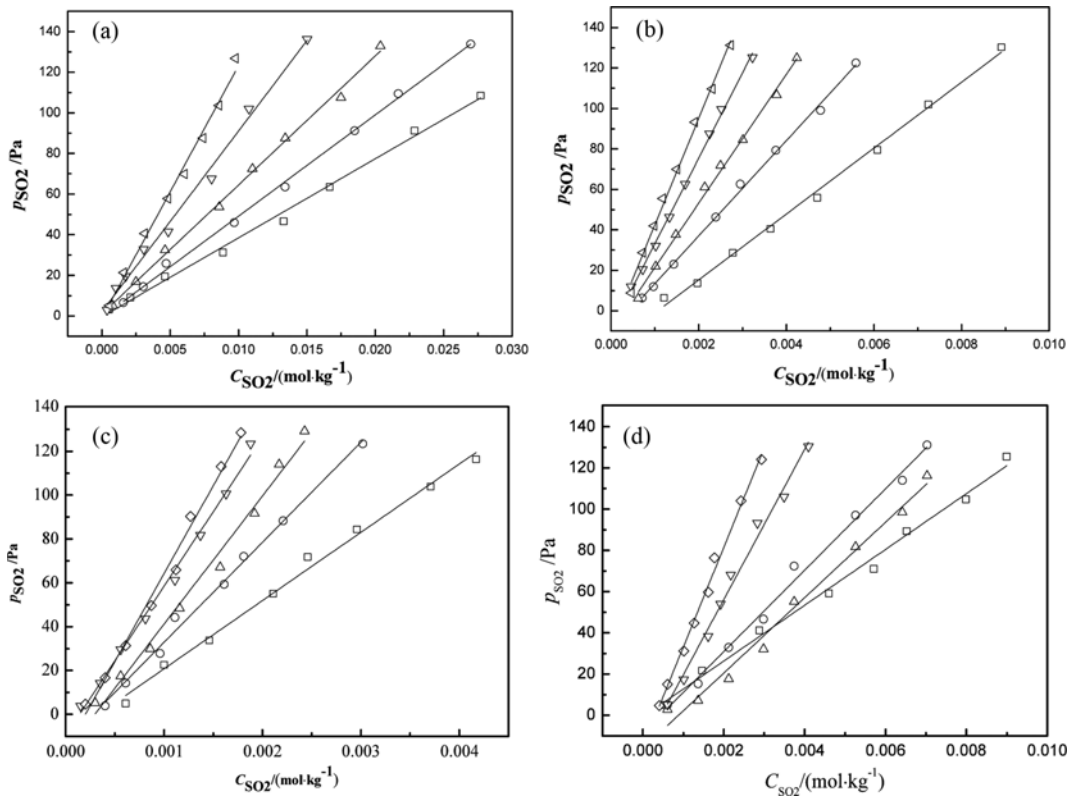

Fig. 4. GLE curves for DEGDME+H_2O+SO_2+N_2 at T=(298.15 to 318.15) K under p=122.7 kPa: (a) w_1=1.00; (b) w_1=0.60; (c) w_1= 0.40; and (d) w_1=0.10. w_1 refers to the mass fraction of DEGDME in mixed solution (DEGDME+H_2O): □, T=298.15 K; ○, T=303.15 K; △, T=308.15 K; ▽, T=313.15 K; and ◇, T=318.15 K.

system DEGDME (1)+H_2O (2)+SO_2 (3)+N_2 (4) are listed in Table S1, and the curves are plotted in Fig. 2. The solubility of dilute SO_2 in DEGDME (1)+H_2O (2) is shown in Fig. 3 when the volume fraction of SO_2 in the gas phase is designed at $y_{SO_2}=7\times10^{-4}$.

From Fig. 2, the equilibrium partial pressure of SO_2 shows a linear response to the concentration of SO_2, which indicates that the absorption processes obeyed Henry's law within the region of investigated pressure. However, the solubility curves did not cross the zero point of coordinate, which implies that the absorption of SO_2 involved both chemical and physical processes [33]. The GLE data of SO_2 in pure H_2O and DEGDME are well consistent with the literature results [17,34-38]. As shown in Fig. 3, the absorption capabilities of the mixture solution presented a descending trend from 1.00 to 0.40 under the given conditions and reached the minimum at 0.40, and then it began to increase. Note that the solubility of SO_2 in the system DEGDME (1)+H_2O (2) presents an extreme minimum at the mass fraction of w_1=(0.40 of 0.0146) mol·kg^{-1} when SO_2 in the gas phase was designed at $y_{SO_2}=7\times10^{-4}$. On the basis of this result, we concluded that there were considerable interactions among DEGDME, H_2O, and SO_2, which were similar to the absorption of SO_2 in EGW [34,35]. Given the optimal solubility of SO_2, the low viscosity and free-flow of the solution, and economic and environmental issues, the DEGDME (1)+H_2O (2) system with w_1=0.10 was considered to possess a high solubility. For this reason, DEGDME (1)+H_2O (2) with w_1=0.10 could be used as a potentially suitable absorbent in the industrial operations for the absorption of SO_2.

On the basis of the GLE data, HLCs were obtained from the slope of the plot of gas phase partial pressure versus the concentration of SO_2 in the liquid phase (Fig. 2). From Fig. 2, the fitting of the dilute SO_2 HLC resulted in a coefficient of R^2>0.99. HLCs were further confirmed by slopes of the fitting lines.

GLE were carried out at T=(293.15, 298.15, 303.15, 308.15 and 313.15) K under p=122.7 kPa, these GLE data are listed in Table S2, and the GLE curves are plotted in Fig. 4. HLC values at different temperatures were obtained in the same way. HLC values increased with increasing temperature. The result can be used to explain that the kinetic energy of SO_2 increased and SO_2 can easily escape from the solvent. The increase in the value of HLC was the fundamental reason that the solubility decreased with increasing temperature. The obtained HLC values and relative deviations at different temperatures are shown in Table 2. These results clearly indicate that the solubility of SO_2 in absorbents decreased with increasing temperature under p=122.7 kPa. All solutions presented high solubility of SO_2, and the sulfur concentration was high in the liquid phase when the SO_2 concentration in the gas phase was zero.

In general, the values of ΔH, ΔS, and ΔG are critical thermodynamic parameters to indicate the internal energy change of a phase reaction. As shown in Table 2, the ΔG, ΔH, and ΔS values had a direct relationship with temperature and clearly reflected the solubility of SO_2 in the absorbent. The ΔH and ΔS values were the

Table 2. Henry's law constant (HLC), Standard Gibbs free energy (ΔG), phase change enthalpy (ΔH) and phase change enthalpy (ΔS) for the absorption processes of SO_2 in DEGDME (1)+H_2O (2) at T=(298.15 to 318.15) K under p=122.7 kPa. w_1 refers to the mass fraction of DEGDME in mixed solution (DEGDME+H_2O)

T/K	$100w_1$	$10^3H'$	ΔG/kJ·mol^{-1}	ΔH/kJ·mol^{-1}	ΔS/J·mol^{-1}·K^{-1}
298.15	100.00	1.67±0.04	−15.7		
303.15	100.00	2.11±0.03	−15.5		
308.15	100.00	2.66±0.07	−15.2	−43.4	−92.0
313.15	100.00	3.69±0.12	−14.6		
318.15	100.00	5.10±0.18	−14.0		
298.15	60.00	6.58±0.15	−12.5		
303.15	60.00	9.40±0.17	−11.8		
308.15	60.00	12.6±0.29	−11.2	−43.4	−104
313.15	60.00	16.5±0.29	−10.7		
318.15	60.00	20.3±0.59	−10.3		
298.15	40.00	12.5±0.39	−10.9		
303.15	40.00	18.0±0.55	−10.1		
308.15	40.00	22.8±0.94	−9.68	−32.3	−72.8
313.15	40.00	26.3±0.82	−9.47		
318.15	40.00	30.6±1.18	−9.22		
298.15	10.00	5.5±0.18	12.9		
303.15	10.00	7.8±0.26	−12.2		
308.15	10.00	11.2±0.33	−11.5	−46.8	−114
313.15	10.00	14.0±0.55	−11.1		
318.15	10.00	18.3±0.53	−10.6		

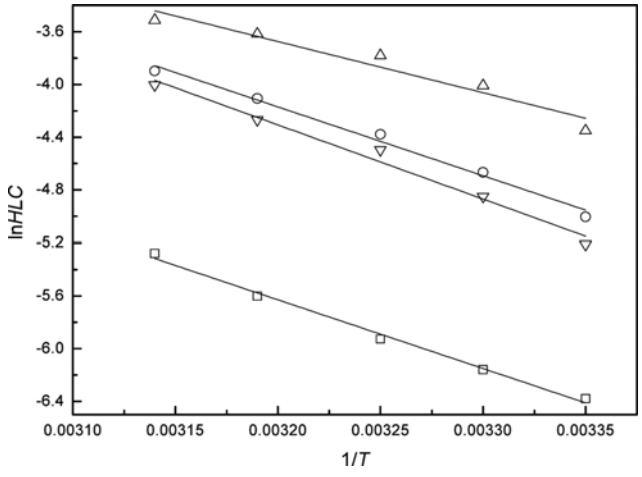

Fig. 5. Temperature dependence of Henry's law constant (HLC) for the absorption process of dilute SO_2 for DEGDME (1)+H_2O (2) DEGDME+H_2O solutions under the system pressure of 122.7 kPa: □, w_1=1.00; ○, w_1=0.60; △, w_1=0.40; ▽, w_1=0.10. w_1 refers to the mass fraction of DEGDME in mixed solution (DEGDME+H_2O).

slope and intercept obtained from the fitting of lnHLC, respectively, as shown in Fig. 5. These results indicated that SO_2 could be captured by these liquids from a mixed gas stream and can be released because of the reversible absorption.

2. Desorption Data of DEGDME (1)+H_2O (2) Containing SO_2

Desorption experiments were performed using N_2 extraction method at the temperature of 308.15 K and 393.15 K with a constant flow of 1 L·min^{-1} for the systems of DEGDME+SO_2, DEGDME+H_2O (w_1=0.60)+SO_2, DEGDME+H_2O (w_1=0.40)+SO_2, and DEGDME+H_2O (w_1=0.10)+SO_2. The corresponding desorption data are listed in Table S3, and their corresponding curves are plotted in Fig. 6. Additionally, the GLE data for recycled systems are listed in Table S4, and their curves are plotted in Fig. 7.

From Fig. 6, it is evident that the concentrations of SO_2 in this system decreased dramatically with increasing temperature, and the desorption rates (>94%) were considerably high. With decreasing concentration of DEGDME, the time taken to reach the desorption equilibrium decreased. The rate of desorption at 393.15 K was higher than that at 308.15 K, which indicates that high temperature is favorable for gas desorption processes. Fig. 7 shows that GLE data were similar to those in Fig. 6, indicating that the recovered solution had the same absorption capacity of SO_2 as the fresh solution. These findings demonstrate that the binary mixture system could be recycled multiple times as the solution for SO_2 absorption and desorption processes with a remarkable stability of SO_2 absorption capacity.

3. Spectral Investigation

3-1. Spectral Properties of H_2O+SO_2 System

The recorded UV spectra of H_2O+SO_2 are shown in Fig. 8, and H_2O was used as the reference solution.

As shown a series of UV-Vis absorption bands were observed with increasing SO_2 concentration. Since SO_2 molecule possesses a Π_3^4 structure [39], it exhibited two typical absorption bands, the $\pi\rightarrow\pi^*$ transition at 220-245 nm and the $n\rightarrow\pi^*$ transition at 270-300 nm. With increasing SO_2 concentration, the absorption band of SO_2 red-shifted from 237 to 244 nm, and the intensity of band

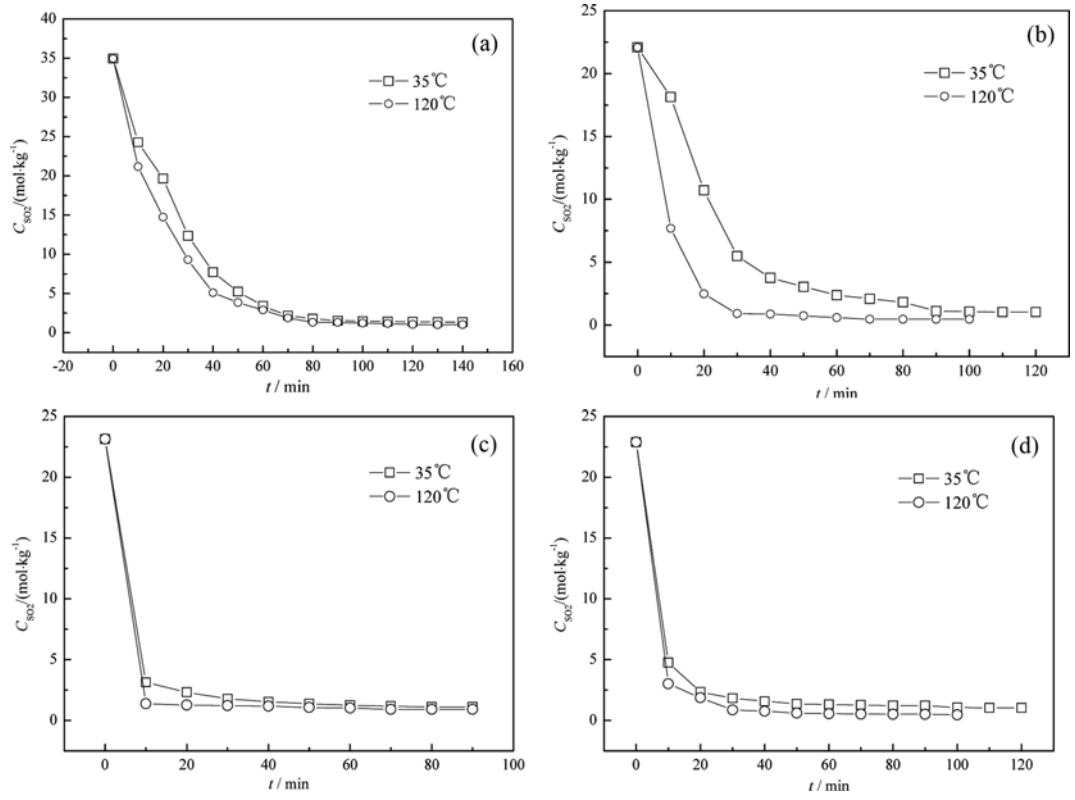

Fig. 6. Curves of SO_2 desorption from the system DEGDME+H_2O at two different temperatures and under atmospheric pressure: (a) w_1=1.00; (b) w_1= 0.60; (c) w_1=0.40; and (d) w_1=0.10.

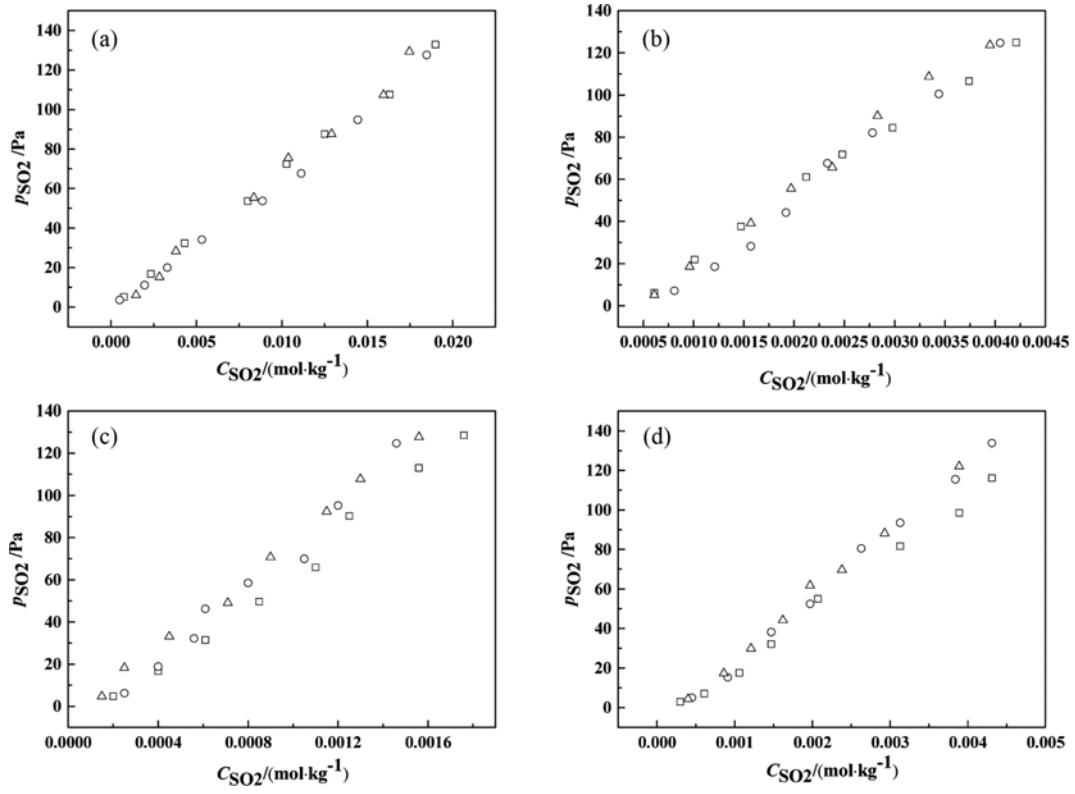

Fig. 7. GLE curves for DEGDME+H_2O+SO_2+N_2 at T=308.15 K and under p=122.7 kPa: (a) w_1=1.00; (b) w_1=0.60; (c) w_1=0.40; (d) w_1=0.10; □, the first absorption; ○, the second absorption; and △, the third absorption. w_1 refers to the mass fraction of DEGDME in mixed solution (DEGDME+H_2O).

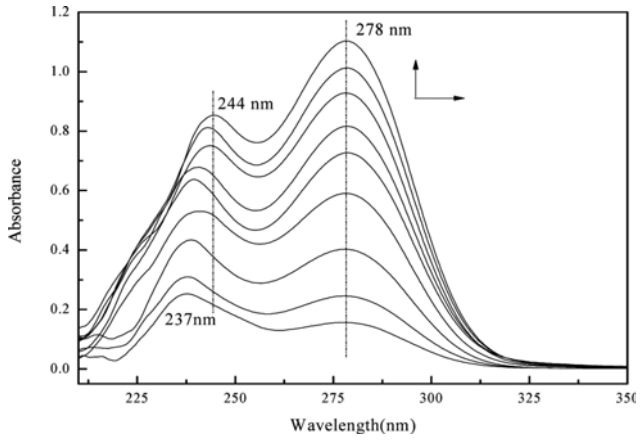

Fig. 8. UV-vis spectral changes at various concentrations of H_2O+ SO_2.

increased concurrently. The reason for this phenomenon is that the oxygen atom in H_2O could slightly affect the sulfur atom in SO_2 through coordination interaction, which decreases the energy of the π system of SO_2, thus facilitating the transition of electron and red-shift of the absorption peak. On the other hand, the absorption peak in the range of 270 to 300 nm only exhibited an increase in the absorption intensity, not together with an increase in the wavelength. This could be attributed to the fact that the unbound electron of the oxygen atom in SO_2 is hardly affected by the interaction between SO_2 and H_2O, thus only exhibiting the intensity change but not the wavelength shift.

The recorded FTIR spectra of H_2O and H_2O+SO_2 are shown in Fig. 9.

FTIR spectra in Fig. 9 clearly show the O-H stretching vibration at 3,444 cm^{-1} and H-O-H bending vibration of H_2O, which did not significantly shift after absorbing SO_2, although three new peaks appeared at 1,333 cm^{-1}, 1,151 cm^{-1}, and 1,051 cm^{-1} after absorption. According to the literature [40,41], the former two bands could be assigned to the symmetric and asymmetric stretching vibration of S=O bond of SO_2. At room temperature, the solubility of SO_2 in water is around 10 g SO_2/100 mL H_2O, which is equal

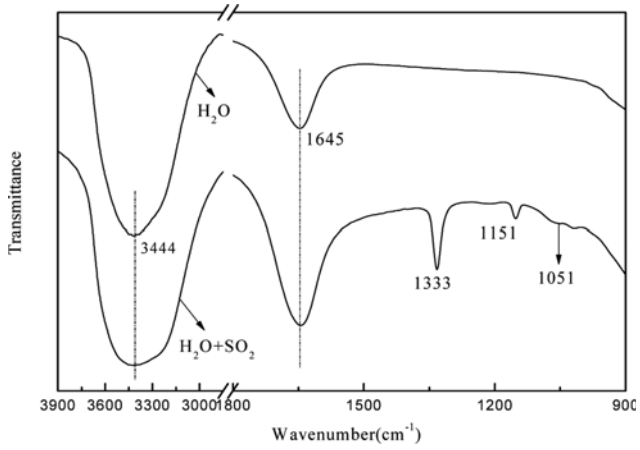

Fig. 9. FTIR Spectra of H_2O+SO_2.

to 1SO_2 molecule dissolved in 35H_2O molecules. Meanwhile, the hydrated $SO_2 \cdot xH_2O$ is also formed by one SO_2 molecule with several H_2O molecules. This indicates even when water is saturated with SO_2, the dominant intermolecular interaction in the SO_2-H_2O solution will still be the intermolecular interaction between H_2O molecules, in which the hydrogen bonding is so strong that it allows H_2O molecules to associate in a large amount. Therefore, it is unlikely that the dissolution of SO_2 could influence the hydrogen bonding between H_2O molecules. As a result, the distinct shift of characteristic H_2O peak in FTIR spectrum was not observed. Moreover, as an acid, H_2SO_3 or hydrated $SO_2 \cdot xH_2O$ could ionize with pKa_1=1.92 and pKa_2=7.18. Under the circumstances, when the water is saturated with SO_2, the amount of HSO_3^- would only account for 10% of that of the entire $SO_2 \cdot xH_2O$ hydrate. Such a small amount revealed on the FTIR spectrum as a weak peak at 1,051 cm^{-1}, which could be easily covered if some other peaks appeared around this range. This further implies that the amount of SO_2 molecule was too little to interrupt the stronger intermolecular interaction among H_2O significantly.

3-2. Spectral Properties of DEGDME+SO_2

The recorded UV spectral changes of DEGDME+SO_2 are shown in Fig. 10, and DEGDME was used as the reference solution.

In DEGDME, the interaction between SO_2 and DEGDME was the same as that in H_2O. Specifically, the $\pi \rightarrow \pi^*$ transition at 223 nm red shifted owing to the coordination effect, whereas the $n \rightarrow \pi^*$ transition at 278 nm did not shift because of the weak interaction between SO_2 and DEGDME. Moreover, the $\pi \rightarrow \pi^*$ transition peak appeared at a short-wavelength compared with that in the H_2O+SO_2 system, which further demonstrated that SO_2 exhibited a weaker interaction with pure H_2O than with pure DEGDME.

The recorded FTIR spectra of DEGDME and DEGDME+SO_2 are shown in Fig. 11.

As shown, the FTIR spectrum of DEGDME changed after absorbing SO_2. Compared with the vibration peak at 1,333 cm^{-1} of SO_2 in H_2O solution, the characteristic symmetric stretching vibration peak of SO_2 appeared at 1,329 cm^{-1}, which implies DEGDME

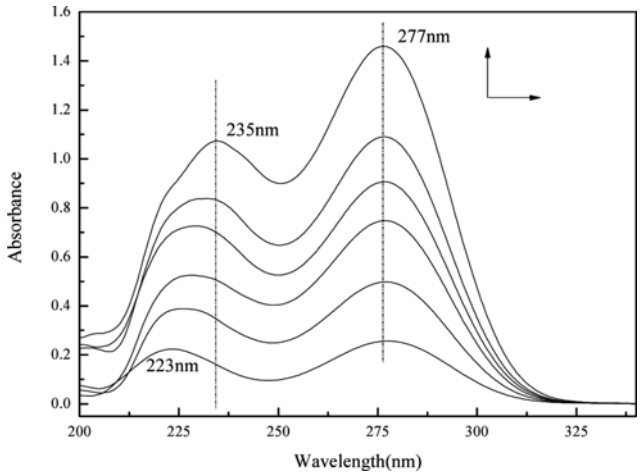

Fig. 10. UV-vis spectral changes at various concentrations of DEGDME+SO_2.

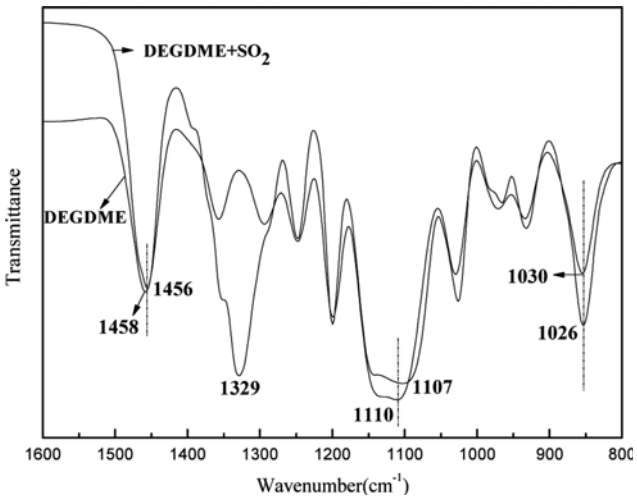

Fig. 11. FTIR spectra of DEGDME+SO_2.

interacted more strongly with SO_2 than with H_2O. It also further demonstrated that the hydrogen bonding interaction among water was more favorable than the interaction between water and SO_2, which caused invariability of O-H bond in IR spectrum after absorption. Meanwhile, there were two peaks at 1,110 cm^{-1} and 1,030 cm^{-1} in DEGDME before absorption of SO_2. According to their peak intensities and structure-function relationship, these two peaks are attributed to the single symmetric C-O-C bond and the double asymmetric C-O-C bond, respectively [42,43]. After absorption of SO_2, these two peaks shifted to the lower wavenumber region of 1,107 cm^{-1} and 1,026 cm^{-1}. This observation indicated the positively charged sulfur atom in SO_2 significantly affected the oxygen atom in DEGDME, which slightly withdrew the electrons in O atom towards S atom, thus weakening the C-O-C bonds and lowering their vibration frequencies. As a result, the wavenumber of these peaks in FTIR decreased. Also, the peak at 1,458 cm^{-1} could be assigned to C-H bending vibration of DEGDME. Because of the electron-withdrawing effect of SO_2 on DEGDME that could be conveyed to adjacent H atoms, the C-H bonds were weakened and stretched, which led to the peak shift towards the lower wavenumber region.

To further elucidate the interaction between SO_2 and DEGDME, we also performed ^{1}H-NMR and ^{13}C-NMR studies for DEGDME before and after absorbing SO_2.

The ^{1}H NMR spectral results of DEGDME+SO_2 are shown in Fig. 12.

Before absorbing SO_2, the triplet at 4.07 ppm (4H), the triplet at 3.98 ppm (4H), and the singlet at 3.82 ppm (6H) corresponded to the two -CH_2- in the middle of the molecule, two -CH_2- adjacent to the methoxy group, and two terminal methoxy groups, respectively. After absorbing SO_2, all peaks shifted towards low field, which is attributed to the positively charged sulfur atom in SO_2. The dipolar interaction between SO_2 and DEGDME enabled the sulfur atoms to bind with the oxygen atoms in DEGDME, thus allowing the sulfur atom to affect the electron density of hydrogen atoms adjacent to the oxygen. This inductive effect resulted in a decrease in the electron density of hydrogen atoms adjacent to the oxygen and a shifting of the chemical shift to the lower field. Moreover, the peaks of -CH_2- tended to merge. The reason is that the positively charged SO_2 induced slightly positive charge on the oxygen atom in DEGDME, which further interrupted the coupling effect of adjacent hydrogen atoms and caused the change of original triplet to doublet and singlet [43].

The ^{13}C NMR spectral results of DEGDME+SO_2 are shown in Fig. 13.

Fig. 13 shows the ^{13}C-NMR spectral change after the absorption of SO_2. Before adsorption of SO_2, the peaks at 75.70 ppm, 74.13 ppm, and 61.83 ppm corresponded to two -CH_2- adjacent to the middle oxygen of the molecule, two -CH_2- adjacent to two terminal methoxy groups, and two methoxy groups, respectively. After absorbing SO_2, all the chemical shifts of the carbon atoms shifted to the high field. This was caused by the weak p-π interaction between oxygen atom in DEGDME with the absorbed SO_2 after the absorption of SO_2, which enhanced the shielding effect of oxygen atom on the adjacent carbon atoms, thus shifting their ^{13}C-NMR peaks to the high field.

The NMR experiments provided valuable information about how DEGDME interacted with SO_2. These results further confirmed that oxygen atom in DEGDME captured the polar and

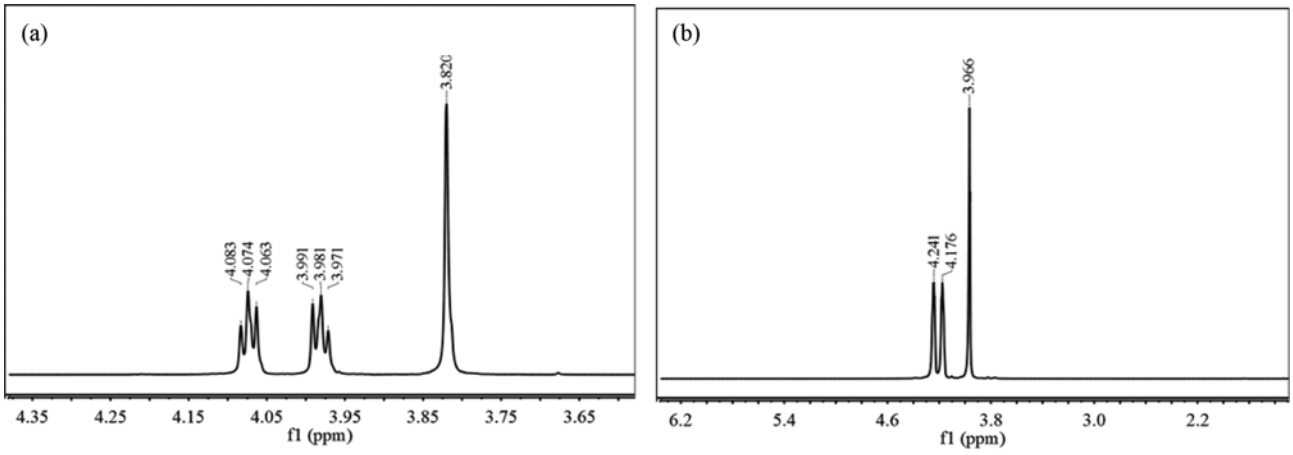

Fig. 12. ^{1}H NMR spectra of DEGDME+SO_2.

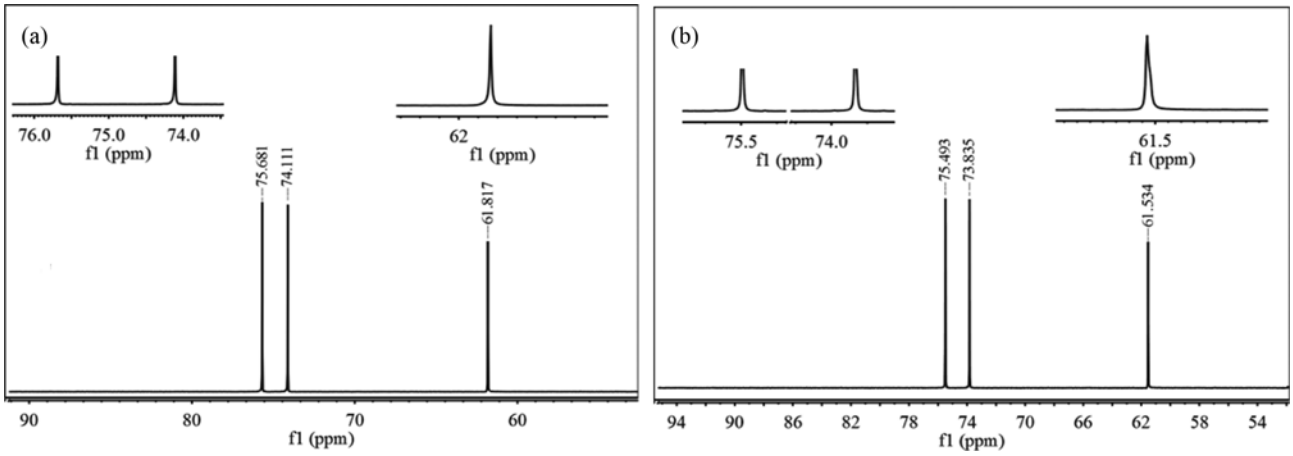

Fig. 13. ^{13}C NMR spectra of DEGDME+SO_2.

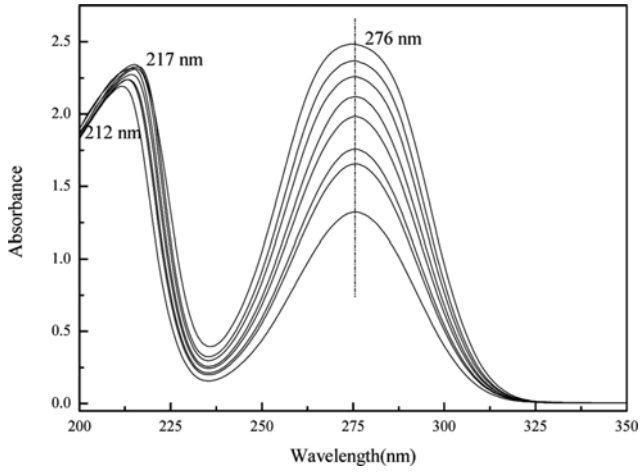

Fig. 14. UV-vis spectral changes at various concentrations of DEGDME+H_2O+SO_2 (w_1=0.1).

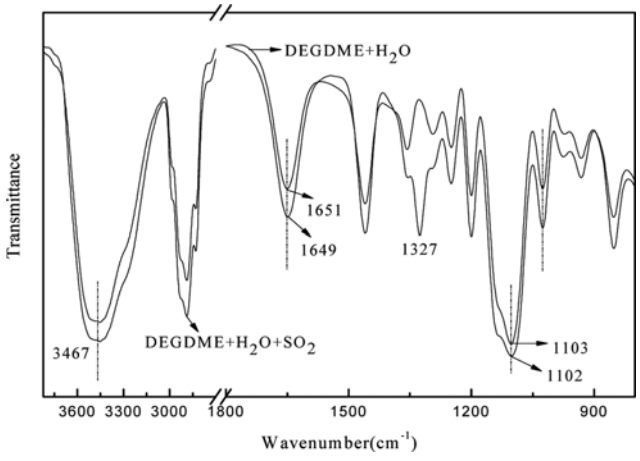

Fig. 15. FTIR spectra of DEGDME+H_2O+SO_2 (w_1=0.1).

acidic SO_2 and formed a stable complex. This specific interaction enabled DEGDME as an efficient and fundamental material in absorbing SO_2, which could be further modified structurally.

3-3. Spectral Properties of DEGDME+H_2O+SO_2

The recorded UV spectral changes of DEGDME+H_2O+SO_2 are shown in Fig. 14, and the DEGDME+H_2O system was used as the reference solution.

Having investigated the spectral properties of single absorption system, we next studied the spectral properties of binary absorption system. It turned out that the binary absorption system exhibited a similar result to pure H_2O or DEGDME absorption system. Specifically, the absorption of SO_2 did not affect the $n\rightarrow\pi^*$ transition, while the peak corresponding to the $\pi\rightarrow\pi^*$ transition red-shifted because of the interaction between SO_2 and H_2O or DEGDME. This further confirmed that oxygen atom in DEGDME is the primary site to interact with SO_2, no matter in H_2O, DEGDME, or H_2O+DEGDME mixture.

The recorded FT-IR spectra of DEGDME and DEGDME+H_2O+SO_2 are shown in Fig. 15.

In IR spectra, the wavenumber of the stretching vibration peak of SO_2 was 1,327 cm^{-1}, which was lower than those of corresponding SO_2 peaks in H_2O and DEGDME systems. According to the previous experimental result, H_2O and DEGDME were miscible, which suggested that the interaction between these two species was strong enough to break their cluster structures and separate them from their initial intermolecular interactions. This is more important for H_2O because the oxygen atom in H_2O has stronger electronegativity than that in DEGDME. Therefore, oxygen in H_2O interacted with the sulfur atom in SO_2 more strongly and then weaken the S-O bonds more significantly. When H_2O molecules were released from their clusters, they tended to capture SO_2 molecules more efficiently than DEGDME, resulting in the most reduced wavenumber of SO_2 in IR spectrum. Meanwhile, the newly formed interaction between H_2O and SO_2 also had some influence on H_2O molecule, which shifted the wavenumber of H_2O bending vibration downwards from 1,651 to 1,649 cm^{-1}. Similarly, the C-O-C bond in DEGDME was also weakened, and the wavenumber of stretching vibration at around 1,100 cm^{-1} decreased. However, the wavenumber corresponding to C-O-C in the binary system did not decrease as much as that of pure DEGDME absorbing system. This was attributed to the fact that SO_2 tended to be captured by H_2O rather than by DEGDME, which reduced the

effect of SO_2 on DEGDME.

CONCLUSION

This paper presented the fundamental investigations on the solubility of SO_2 in various aqueous DEGDME solutions with different compositions. The GLE data showed that the absorption capabilities of DEGDME+H_2O mixture solution exhibited a decreasing trend with decreasing DEGDME concentration in the mass fraction range of w_1=(1.00-0.40), an extreme minimum at the mass fraction of w_1=0.40, and an increasing trend in the range of w_1=(0.40-0.05). The solubility of SO_2 in w_1=0.40 DEGDME (1)+H_2O (2) system exhibited an extreme maximum of 1.76 mol·m^{-3} when SO_2 in the gas phase was designed at $y_{SO_2}=7\times10^{-4}$. The solubility of SO_2 in DEGDME (1)+H_2O (2) system decreased with increasing temperature. The dissolving process of SO_2 in DEGDME+H_2O mixtures was spontaneous and exothermic under the given conditions.

The data of desorption experiment demonstrated that the binary mixture of DEGDME (1)+H_2O (2) could be used as an efficient desulfurization solution, and the corresponding desorption rate of SO_2 in the mixture was over 94%. The regenerated solution showed the similar absorption capacity of SO_2 compared with the fresh solution. From the spectral analyses, it was concluded that both H_2O and DEGDME interact with SO_2 mainly through their oxygen atoms. Moreover, the strong hydrogen bonding formed in water could prevent oxygen atom from binding with SO_2 tightly. Once the hydrogen bonding is collapsed by mixing with DEGDME, both H_2O and DEGDME are able to absorb SO_2 efficiently and reversibly.

ACKNOWLEDGEMENTS

This work was supported by the National Natural Science Foundation of China (21166017), Program for New Century Excellent Talents in University (NCET-12-1017), the Inner Mongolia Science and Technology Key Projects, the Program for Grassland Excellent Talents of Inner Mongolia Autonomous Region, and training plan of academic backbone in youth of Inner Mongolia University of Technology.

SUPPORTING INFORMATION

Additional information as noted in the text. This information is available via the Internet at http://www.springer.com/chemistry/journal/11814.

REFERENCES

1. Y. Zhao, Y. H. Han and C. Chen, *Ind. Eng. Chem. Res.*, **51**, 480 (2012).
2. J. Zhi, X. Yu, J. Bao, X. Jiang and H, Yang, *Korean J. Chem. Eng.*, **33**(6), 1823 (2016).
3. Y. G. Zhou, M. C. Zhang, D. F. Wang and L. Wang, *Ind. Eng. Chem. Res.*, **44**, 8830 (2005).
4. M. A. Siddiqi, J. Krissmann, P. Peters-Gerth, M. Luckas and K. Lucas, *J. Chem. Thermodyn.*, **28**, 685 (1996).
5. S. Pereda, K. Thomsen and P. Rasmussen, *Chem. Eng. Sci.*, **55**, 2663 (2000).
6. J. Krissmann, M. A. Siddiqi and K. Lucas, *Fluid Phase Equilib.*, **141**, 221 (1997).
7. K. Zimmermann, C. Pasel, M. Luckas and J. Herbell, *Fluid Phase Equilib.*, **279**, 105 (2009).
8. A. Valtz, C. Coquelet and D. Richon, *Int. J. Thermophys.*, **25**, 1695 (2004).
9. J. B. Zhang, P. Y. Zhang, G. H. Chen, F. Han and X. H. Wei, *J. Chem. Eng. Data*, **53**, 1479 (2008).
10. J. B. Zhang, L. H. Liu, T. R. Huo, Z. Y. Liu, T. Zhang and X. H. Wei, *J. Chem. Thermodyn.*, **43**, 1463 (2011).
11. N. Zhang, J. B. Zhang, Y. F. Zhang, J. Bai, T. R. Huo and X. H. Wei, *Fluid Phase Equilibr.*, **313**, 7 (2012).
12. B. Guo, T. Zhao, F. Sha, F. Zhang, Q. Li and J. Zhang, *Korean J. Chem. Eng.*, **33**(6), 1883 (2016).
13. S. F. Sciamanna and L. Scott, *Ind. Eng. Chem. Res.*, **27**, 492 (1988).
14. A. L. Revelli, F. Mutelet and J. N. Jaubert, *J. Phys. Chem. B*, **114**, 12908 (2010).
15. S. Y. Sun, Y. X. Yan, Z. C. Sun, Q. X. Xu and X. H. Wei, *RSC Adv.*, **5**, 8706 (2015).
16. Y. X. Niu, F. Gao, S. Y. Sun, J. B. Xiao and X. H. Wei, *Fluid Phase Equilibr.*, **344**, 65 (2013).
17. Y. Chang, J. Zhang, Q. Li, L, Li, B. Guo and T. Zhao, *Korean J. Chem. Eng.*, **31**(2), 2245 (2014).
18. A. Douabul and J. Riley, *J. Chem. Eng. Data*, **24**, 274 (1979).
19. B. Rumpf and G. Maurer, *Fluid Phase Equilibr.*, **81**, 241 (1992).
20. H. Li, D. Z. Liu, F. and A. Wang, *J. Chem. Eng. Data*, **47**, 772 (2002).
21. H. Li, X. Jiao and W. Chen, *Phys. Chem. Liq.*, **52**, 349 (2014).
22. A. E. Rabe and J. F. Harris, *J. Chem. Eng. Data*, **8**, 333 (1963).
23. J. Vosolsobe, S. Simecek, J. Michalek and B. Kadler, *Chem. Prum.*, **15**, 401 (1965).
24. Q. X. Xu, S. Y. Sun, G. J. Lan, J. B. Bai, J. B. Zhang and X. H. Wei, *J. Chem. Eng. Data*, **60**, 2 (2015).
25. C. Dethlefsen and A. Hvidt, *J. Chem. Thermodyn.*, **17**, 193 (1985).
26. T. M. Aminabhavi and B. Gopalakrishna, *J. Chem. Eng. Data*, **40**, 462 (1995).
27. J. Rodriguez-Sevilla, M. Alvarez, G. Limiñana and M. C. Diaz, *J. Chem. Eng. Data*, **47**, 1339 (2002).
28. J. L. Anthony, E. J. Maginn and J. F. Brennecke, *J. Phys. Chem. B*, **106**, 7315 (2002).
29. A. Henni, P. Tontiwachwuthikul and A. Chakma, *Can. J. Chem. Eng.*, **83**, 358 (2005).
30. H. A. Bamford, D. L. Poster and J. E. Baker, *Environ. Toxicol. Chem.*, **18**, 1905 (1999).
31. X. C. Fu and W. X. Shen, Physical Chemistry, 5th Ed. Higher Press, Beijing (2005).
32. M. Jin, Y. Hou, W. Wu, S. Ren, S. Tian, L. Xiao and Z. Lei, *J. Phys. Chem. B*, **115**, 6585 (2011).
33. J. B. Zhang, F. Han, X. H. Wei, L. K. Shui and H. Gong, *Ind. Eng. Chem. Res.*, **49**, 2025 (2010).
34. A. Douabul and J. Riley, *J. Chem. Eng. Data*, **24**, 274 (1979).
35. G. Alenezi, H. Ettouney, E. A. Hisham and F. Naglaa, *Ind. Eng. Chem. Res.*, **40**, 1434 (2001).

36. A. C. Shaw, M. A. Romero and R. H. Elder, *Int. J. Hydrogen Energy*, **36**, 4749 (2011).
37. S. Augusta, *Anal. Chem.*, **45**, 1744 (1973).
38. A. Lasgabaster, M. J. Abad and L. Barral, *Eur. Polym. J.*, **42**, 3121 (2006).
39. M. H. H. van Dam, A. S. Lamine and D. Roizard, *Ind. Eng. Chem. Res.*, **36**, 4628 (1997).
40. M. Yarra, B. N. P. Rachapudi and L. K. S. Mallampalli, *Eur. J. Inorg. Chem.*, **5**, 260 (2014).
41. R. Frech and W. W. Huang, *Macromolecules*, **28**, 1246 (1994).
42. D. H. William and I. Fleming, Spectroscopy Methods in Org. chemistry, 6th Ed. New York, McGraw-Hill (2005).
43. X. Y. Zhao and X. Y. Sun, Spectral identification for organic molecular structure, 2th Ed. Beijing (2010).

Supporting Information

Experimental solubility and absorption mechanism of dilute SO_2 in aqueous diethylene glycol dimethyl ether solution

Qiuxia Xu*, Jianbai Xiao, Jianbin Zhang*,†, and Xionghui Wei**,†**

*College of Chemical Engineering, Inner Mongolia University of Technology, Huhhot 010051, China
**Department of Applied Chemistry, College of Chemistry & Molecular Engineering, Peking University, Beijing 100871, China
(*Received 2 April 2016 • accepted 18 July 2016*)

Table S1. GLE Data for DEGDME (1)+H_2O (2)+SO_2 (3)+N_2 (4) at 308.15 K and under 122.7 kPa[a,b]

$100w_1$	C_{SO_2}/mol·kg^{-1}	p_{SO_2}/Pa	$10^6y_{SO_2}$	$100w_1$	C_{SO_2}/mol·kg^{-1}	p_{SO_2}/Pa	$10^6y_{SO_2}$
0.00	0.00096	5.3	43	50.00	0.00210	63.1	515
0.00	0.00157	14.9	122	50.00	0.00251	82.7	674
0.00	0.00213	35.5	289	50.00	0.00326	114.2	931
0.00	0.00299	52.1	425	50.00	0.00351	129.2	1054
0.00	0.00365	74.7	609	60.00	0.00061	6.1	50
0.00	0.00481	91.7	748	60.00	0.00101	21.9	179
0.00	0.00548	112.3	916	60.00	0.00147	37.6	306
0.00	0.00624	132.2	1077	60.00	0.00212	61.1	498
10.00	0.00030	2.9	23	60.00	0.00248	71.8	585
10.00	0.00061	7.2	58	60.00	0.00298	84.5	689
10.00	0.00106	17.6	144	60.00	0.00374	106.6	869
10.00	0.00147	32.1	262	60.00	0.00421	124.9	1019
10.00	0.00207	55.1	449	70.00	0.00112	6.5	53
10.00	0.00313	81.7	666	70.00	0.00204	18.8	154
10.00	0.00389	98.5	803	70.00	0.00266	35.1	286
10.00	0.00431	116.2	947	70.00	0.00389	50.8	414
20.00	0.00061	6.8	55	70.00	0.00465	61.9	505
20.00	0.00101	17.0	139	70.00	0.00532	81.3	663
20.00	0.00162	38.7	315	70.00	0.00675	105.8	863
20.00	0.00191	55.1	449	70.00	0.00747	116.2	947
20.00	0.00216	67.9	554	80.00	0.00098	5.1	42
20.00	0.00282	91.3	744	80.00	0.00275	19.0	155
20.00	0.00348	111.0	905	80.00	0.00487	44.7	364
20.00	0.00444	145.1	1183	80.00	0.00648	72.1	588
30.00	0.00040	4.9	40	80.00	0.00767	87.6	714
30.00	0.00061	13.8	112	80.00	0.00923	104.4	851
30.00	0.00095	28.7	234	80.00	0.01001	118.5	966
30.00	0.00125	42.9	350	80.00	0.01229	145.1	1183
30.00	0.00161	59.3	483	90.00	0.00085	6.0	49
30.00	0.00186	70.4	574	90.00	0.00206	11.0	90
30.00	0.00216	86.4	705	90.00	0.00433	25.7	210
30.00	0.00262	114.2	931	90.00	0.00733	51.0	416
40.00	0.00030	5.2	42	90.00	0.01008	70.9	578
40.00	0.00056	17.5	143	90.00	0.01250	87.5	714
40.00	0.00085	29.9	244	90.00	0.01388	104.4	851
40.00	0.00115	48.4	394	90.00	0.01614	126.6	1032
40.00	0.00156	67.1	547	100.00	0.00081	5.1	42

Table S1. Continued

$100w_1$	C_{SO_2}/mol·kg^{-1}	p_{SO_2}/Pa	$10^6y_{SO_2}$	$100w_1$	C_{SO_2}/mol·kg^{-1}	p_{SO_2}/Pa	$10^6y_{SO_2}$
40.00	0.00191	91.6	747	100.00	0.00248	16.8	137
40.00	0.00216	114.0	929	100.00	0.00458	32.4	264
40.00	0.00241	129.2	1054	100.00	0.00850	53.7	438
50.00	0.00051	9.6	78	100.00	0.01092	72.4	590
50.00	0.00090	18.7	153	100.00	0.01329	87.5	713
50.00	0.00141	37.4	305	100.00	0.01732	107.6	877
50.00	0.00181	50.5	412	100.00	0.02017	132.9	1083

[a]Standard uncertainties u are $u(w_1)=0.01$, $u(T)=0.01$ K, and $u(p)=0.10$ kPa. Relative expanded uncertainties are $U_r(C_{SO_2})=0.60\%$ and $U_r(y_{SO_2})=2.50\%$

[b]w_1: mass fraction of DEGDME in mixed solution. C_{SO2}: the concentration of SO_2 in the liquid phase. y_{SO_2}: the volume fraction of SO_2. p_{SO_2}: the volume fraction of SO_2 in the gas phase

Table S2. GLE data for DEGDME (1)+H_2O (2)+SO_2 (3)+N_2 (4) at five different temperatures and under p=122.7 kPa[a,b]

T/K	C_{SO_2}/mol·kg^{-1}	p_{SO_2}/Pa	$10^6y_{SO_2}$	T/K	C_{SO_2}/mol·kg^{-1}	p_{SO_2}/Pa	$10^6y_{SO_2}$
			$100w_1$=100				
298.15	0.00054	3.2	26	308.15	0.01102	72.4	590
298.15	0.00210	9.1	74	308.15	0.01342	87.5	713
298.15	0.00463	19.3	157	308.15	0.01749	107.6	877
298.15	0.00887	31.2	255	308.15	0.02037	132.9	1083
298.15	0.01329	46.6	380	313.15	0.00038	2.9	24
298.15	0.01667	63.5	517	313.15	0.00104	13.6	111
298.15	0.02287	91.2	744	313.15	0.00175	19.5	159
298.15	0.02771	108.5	885	313.15	0.00306	32.8	267
303.15	0.00157	6.6	54	313.15	0.00486	41.5	338
303.15	0.00303	14.4	117	313.15	0.00803	67.6	551
303.15	0.00471	25.8	210	313.15	0.01076	101.9	831
303.15	0.00968	45.9	375	313.15	0.01502	136.2	1110
303.15	0.01341	63.5	518	318.15	0.00055	5.2	43
303.15	0.01849	91.2	743	318.15	0.00160	21.3	174
303.15	0.02168	109.4	892	318.15	0.00313	40.6	331
303.15	0.02698	133.8	1091	318.15	0.00483	57.8	471
308.15	0.00082	5.1	42	318.15	0.00604	69.8	569
308.15	0.00250	16.8	137	318.15	0.00740	87.5	713
308.15	0.00462	32.4	264	318.15	0.00857	103.6	844
308.15	0.00858	53.7	438	318.15	0.00977	126.8	1034
			$100w_1$=60				
298.15	0.00121	6.4	52	308.15	0.00250	71.8	585
298.15	0.00197	13.6	111	308.15	0.00301	84.5	689
298.15	0.00278	28.6	233	308.15	0.00378	106.6	869
298.15	0.00364	40.5	330	308.15	0.00424	124.9	1019
298.15	0.00471	55.9	456	313.15	0.00046	11.9	97
298.15	0.00608	79.5	648	313.15	0.00072	20.4	166
298.15	0.00724	101.9	831	313.15	0.00102	32.1	262
298.15	0.00891	130.2	1061	313.15	0.00133	46.3	377
303.15	0.00071	6.3	51	313.15	0.00169	62.6	510
303.15	0.00097	11.9	97	313.15	0.00225	87.5	713
303.15	0.00143	23.0	188	313.15	0.00252	99.6	812
303.15	0.00239	46.3	377	313.15	0.00323	125.2	1021
303.15	0.00295	62.6	510	318.15	0.00046	8.8	72
303.15	0.00376	79.3	646	318.15	0.00072	28.7	234

Table S2. Continued

T/K	C_{SO_2}/mol·kg^{-1}	p_{SO_2}/Pa	$10^6 y_{SO_2}$	T/K	C_{SO_2}/mol·kg^{-1}	p_{SO_2}/Pa	$10^6 y_{SO_2}$
303.15	0.00478	99.0	808	318.15	0.00098	42.0	342
303.15	0.00559	122.5	999	318.15	0.00118	55.5	452
308.15	0.00062	6.1	50	318.15	0.00150	69.9	570
308.15	0.00102	21.9	179	318.15	0.00191	93.2	760
308.15	0.00148	37.6	306	318.15	0.00231	109.6	894
308.15	0.00214	61.1	498	318.15	0.00273	131.3	1070
			$100w_1$=40				
298.15	0.00061	4.9	40	308.15	0.00157	67.1	547
298.15	0.00100	22.6	184	308.15	0.00192	91.6	747
298.15	0.00146	33.7	275	308.15	0.00217	114.0	929
298.15	0.00211	55.1	449	308.15	0.00243	129.2	1054
298.15	0.00246	71.8	585	313.15	0.00015	3.9	32
298.15	0.00296	84.3	688	313.15	0.00035	14.2	116
298.15	0.00371	103.8	846	313.15	0.00056	29.6	242
298.15	0.00417	116.3	948	313.15	0.00081	43.7	356
303.15	0.00040	3.9	32	313.15	0.00111	61.2	499
303.15	0.00061	14.2	116	313.15	0.00137	81.7	666
303.15	0.00096	27.8	227	313.15	0.00163	100.6	820
303.15	0.00111	44.2	360	313.15	0.00188	123.4	1005
303.15	0.00161	59.3	483	318.15	0.00020	4.7	38
303.15	0.00181	72.0	587	318.15	0.00040	16.7	136
303.15	0.00221	88.3	720	318.15	0.00061	31.4	256
303.15	0.00302	123.4	1006	318.15	0.00087	49.6	404
308.15	0.00030	5.2	42	318.15	0.00112	65.9	537
308.15	0.00056	17.5	143	318.15	0.00127	90.3	736
308.15	0.00086	29.9	244	318.15	0.00158	113.0	921
308.15	0.00116	48.4	394	318.15	0.00178	128.5	1047
			$100w_1$=10				
298.15	0.00051	4.9	41	308.15	0.00208	55.1	449
298.15	0.00147	21.6	176	308.15	0.00314	81.7	666
298.15	0.00288	41.1	335	308.15	0.00391	98.5	803
298.15	0.00461	59.1	482	308.15	0.00432	116.2	947
298.15	0.00572	71.0	579	313.15	0.00061	5.2	43
298.15	0.00653	89.3	728	313.15	0.00102	17.4	142
298.15	0.00800	104.8	854	313.15	0.00163	38.3	313
298.15	0.00901	125.4	1023	313.15	0.00193	53.9	440
303.15	0.00061	5.1	42	313.15	0.00218	68.1	556
303.15	0.00136	15.3	125	313.15	0.00285	93.3	760
303.15	0.00213	32.9	268	313.15	0.00351	106.0	864
303.15	0.00299	46.6	380	313.15	0.00411	130.3	1062
303.15	0.00375	72.4	590	318.15	0.00040	4.7	38
303.15	0.00527	97.0	791	318.15	0.00061	15.1	123
303.15	0.00644	113.9	929	318.15	0.00102	31.1	254
303.15	0.00705	131.1	1069	318.15	0.00127	44.7	364
308.15	0.00030	2.9	23	318.15	0.00163	59.7	487
308.15	0.00061	7.1	58	318.15	0.00178	76.4	623
308.15	0.00107	17.6	144	318.15	0.00245	104.0	848
308.15	0.00148	32.1	262	318.15	0.00295	124.0	1011

[a]Standard uncertainties u are u(w_1)=0.01, u(T)=0.01 K, and u(p)=0.10 kPa. Relative expanded uncertainties are $U_r(C_{SO_2})$=0.60% and $U_r(y_{SO_2})$ =2.50%

[b]w_1: mass fraction of DEGDME in mixed solution. C_{SO_2}: the concentration of SO_2 in the liquid phase. y_{SO_2}: the volume fraction of SO_2. p_{SO_2}: the volume fraction of SO_2 in the gas phase

Table S3. Data of SO_2 desorption from the system DEGDME (1)+H_2O (2) at two different temperatures and under atmospheric pressure

t/min	C_{SO_2}/mol·m^{-3} (35 °C)	C_{SO_2}/mol·m^{-3} (120 °C)	t/min	C_{SO_2}/mol·m^{-3} (35 °C)	C_{SO_2}/mol·m^{-3} (120 °C)
	DEGDME			100w_1=60 DEGDME (1)+H_2O (2)	
0	34.95	34.95	0	22.08	22.08
10	24.27	21.17	10	18.12	7.69
20	19.65	14.72	20	10.71	2.47
30	12.34	9.29	30	5.48	0.91
40	7.72	5.08	40	3.76	0.86
50	5.23	3.86	50	3.05	0.75
60	3.40	2.89	60	2.39	0.59
70	2.18	1.88	70	2.08	0.47
80	1.78	1.32	80	1.83	0.47
90	1.52	1.32	90	1.12	0.46
100	1.46	1.22	100	1.07	0.46
110	1.42	1.17	110	1.03	
120	1.39	1.07	120	1.03	
130	1.35	1.02			
140	1.35	1.02			
Desorption rate	96.1%	97.1%	Desorption rate	95.3%	97.9%
	100w_1=40 DEGDME (1)+H_2O (2)			100w_1=10 DEGDME(1)+H_2O(2)	
0	23.14	23.14	0	22.88	22.88
10	3.13	1.37	10	4.76	3.02
20	2.32	1.27	20	2.34	1.86
30	1.78	1.22	30	1.83	0.86
40	1.53	1.17	40	1.57	0.76
50	1.38	1.07	50	1.36	0.61
60	1.25	1.02	60	1.31	0.56
70	1.18	0.91	70	1.27	0.53
80	1.12	0.92	80	1.22	0.51
90	1.12	0.91	90	1.22	0.51
Desorption rate	95.1%	96.1%	Desorption rate	94.7%	97.7%

Table S4. GLE Data of repeated absorption for DEGDME (1)+H_2O (2)+SO_2 (3)+N_2 (4) at T=308.15 K and under p=122.66 kPa[a,b]

$100w_1$	C_{SO_2}/mol·kg^{-1}	p_{SO_2}/Pa	$10^6y_{SO_2}$	$100w_1$	C_{SO_2}/mol·kg^{-1}	p_{SO_2}/Pa	$10^6y_{SO_2}$
100.00[a]	0.00076	5.1	42	40.00[a]	0.00020	4.7	38
100.00[a]	0.00233	16.8	137	40.00[a]	0.00040	16.7	136
100.00[a]	0.00431	32.4	264	40.00[a]	0.00061	31.4	256
100.00[a]	0.00800	53.7	438	40.00[a]	0.00085	49.6	404
100.00[a]	0.01028	72.4	590	40.00[a]	0.00110	65.9	537
100.00[a]	0.01251	87.5	713	40.00[a]	0.00125	90.3	736
100.00[a]	0.01631	107.6	877	40.00[a]	0.00156	113.0	921
100.00[a]	0.01899	132.9	1083	40.00[a]	0.00176	128.5	1047
100.00[b]	0.00051	3.6	30	40.00[b]	0.00025	6.2	51
100.00[b]	0.00197	11.1	90	40.00[b]	0.00040	18.8	153
100.00[b]	0.00330	20.0	163	40.00[b]	0.00056	32.2	263
100.00[b]	0.00532	34.1	278	40.00[b]	0.00061	46.2	377
100.00[b]	0.00887	53.7	438	40.00[b]	0.00080	58.5	477
100.00[b]	0.01114	67.6	551	40.00[b]	0.00105	69.9	570
100.00[b]	0.01444	94.8	773	40.00[b]	0.00120	95.2	776
100.00[b]	0.01848	127.6	1040	40.00[b]	0.00146	124.7	1016
100.00[c]	0.00147	6.0	49	40.00[c]	0.00015	4.7	38
100.00[c]	0.00284	15.2	124	40.00[c]	0.00025	18.3	149
100.00[c]	0.00380	28.3	231	40.00[c]	0.00045	33.1	270
100.00[c]	0.00836	55.4	451	40.00[c]	0.00071	49.0	399
100.00[c]	0.01038	75.5	615	40.00[c]	0.00090	70.8	577
100.00[c]	0.01291	87.6	714	40.00[c]	0.00115	92.4	753
100.00[c]	0.01595	107.4	876	40.00[c]	0.00130	107.8	879
100.00[c]	0.01747	129.3	1054	40.00[c]	0.00156	127.7	1041
60.00[a]	0.00061	6.1	50	10.00[a]	0.00030	2.9	23
60.00[a]	0.00101	21.9	179	10.00[a]	0.00061	7.1	58
60.00[a]	0.00147	37.6	306	10.00[a]	0.00106	17.6	144
60.00[a]	0.00212	61.1	498	10.00[a]	0.00147	32.1	262
60.00[a]	0.00248	71.8	585	10.00[a]	0.00207	55.1	449
60.00[a]	0.00298	84.5	689	10.00[a]	0.00313	81.7	666
60.00[a]	0.00374	106.6	869	10.00[a]	0.00389	98.5	803
60.00[a]	0.00421	124.9	1019	10.00[a]	0.00431	116.2	947
60.00[b]	0.00081	7.1	58	10.00[b]	0.00045	5.0	41
60.00[b]	0.00121	18.5	151	10.00[b]	0.00091	15.3	125
60.00[b]	0.00157	28.2	230	10.00[b]	0.00147	38.2	311
60.00[b]	0.00192	44.2	360	10.00[b]	0.00197	52.5	428
60.00[b]	0.00233	67.6	551	10.00[b]	0.00263	80.5	657
60.00[b]	0.00278	82.1	669	10.00[b]	0.00313	93.5	762
60.00[b]	0.00344	100.5	819	10.00[b]	0.00384	115.5	942
60.00[b]	0.00405	124.7	1016	10.00[b]	0.00431	133.8	1091
60.00[c]	0.00061	5.1	42	10.00[c]	0.00040	4.4	36
60.00[c]	0.00096	18.6	152	10.00[c]	0.00086	17.3	141
60.00[c]	0.00157	39.2	320	10.00[c]	0.00121	29.9	244
60.00[c]	0.00197	55.6	454	10.00[c]	0.00162	44.3	361
60.00[c]	0.00238	65.6	535	10.00[c]	0.00197	61.8	504
60.00[c]	0.00283	90.1	734	10.00[c]	0.00238	69.7	568
60.00[c]	0.00334	108.7	886	10.00[c]	0.00293	88.2	719
60.00[c]	0.00395	123.7	1008	10.00[c]	0.00389	122.1	995

[a]Standard uncertainties u are u(w_1)=0.01, u(T)=0.01 K, and u(p)=0.10 kPa. Relative expanded uncertainties are $U_r(C_{SO_2})$=0.60% and $U_r(y_{SO_2})$ =2.50%

[b]w_1: mass fraction of DEGDME in mixed solution. C_{SO_2}: the concentration of SO_2 in the liquid phase. y_{SO_2}: the volume fraction of SO_2. p_{SO_2}: the volume fraction of SO_2 in the gas phase